III. Idealized geometries were used to provide a bridge among the known experimental structures. The geometry of the CH_2 unit was fixed for its transits on the energy surfaces. The bond distances used throughout were C-H = 1.09 Å, M-C = 2.083 Å, M-Cl = 2.3 Å, M-P = 2.28 Å, P-H = 1.42 Å, and C-C (metallacyclobutane) = 1.535 Å. The geometry of the planar metallacyclobutane had ∠C-M-C = 67.3°, ∠M-C-C = 97.6°, and ∠C-C-C = 97.5°.

(28) Ammeter, J. H.; Bürgi, H. B.; Thibeault, J. C.; Hoffmann, R. *J. Am. Chem. Soc.* **1978**, *100*, 3686-3692.

Registry No. $(Cl)_3Pt(CH_2)_3^{3-}$, 85957-26-2; $(Cl)_3Pt(CH_2)_3^-$, 85957-25-1; $(Cl)_3Pt(CH_2)_3^+$, 85957-27-3; $(Cl)_3Pt(CH_2)_3^{3+}$, 85957-28-4; $(Cl)_3W(CH_2)_3^{3-}$, 85957-29-5; $(Cl)_3W(CH_2)_3^-$, 85957-30-8; $(Cl)_3W(CH_2)_3^+$, 85957-31-9.

The Mechanism of Fe-EDTA Catalyzed Superoxide Dismutation[1]

Christopher Bull, Gregory J. McClune,† and James A. Fee*

Contribution from the Biophysics Research Division and Department of Biological Chemistry, The University of Michigan, Ann Arbor, Michigan 48109. *Received February 4, 1983*

Abstract: The catalysis of superoxide dismutation ($2O_2 + 2H^+ \rightarrow O_2 + H_2O_2$) by Fe^{3+}-EDTA and Fe^{2+}-EDTA has been examined. Potentiometric and spectrophotometric titrations of Fe^{3+}-EDTA revealed an ionization at $pK_a = 7.6$ consistent with the ionization of a bound water molecule. No other ionizations were detected below pH 10.7. Potentiometric titration of Fe^{2+}-EDTA revealed no ionizations in the pH range 5-11. We have studied the kinetic behavior of three reactions which constitute a catalytic cycle for O_2^- dismutation: $O_2^- + Fe^{3+}$-EDTA $\rightleftharpoons Fe^{2+}$-EDTA $+ O_2$ (reaction 4), $O_2^- + Fe^{2+}$-EDTA $\rightleftharpoons Fe^{3+}$-EDTA-$O_2^{2-}$ (reaction 5), and $H_2O_2 + Fe^{3+}$-EDTA-$OH^- \rightleftharpoons Fe^{3+}$-EDTA-$O_2^{2-} + H_3O^+$ (reaction 6). Combining our data with that available in the literature we find that between pH 7 and pH 11 reaction 4 is described by the expression $k_{obsd} \approx 2 \times 10^6$ M^{-1} s^{-1} $[H^+/(H^+ + K_a)]$ where $pK_a \approx 7.6$. Reaction 5 appears to be independent of pH and occurs with a velocity constant of 10^6-10^7 M^{-1} s^{-1}. A mechanism has been derived for reaction 6 which accounts for the pH dependence of the individual rate constants, general-acid catalysis, and the pH dependence of the formation constant. The breakdown of the peroxo complex is catalyzed by both specific and general acids, and $k_{-6}/[H^+] \simeq 10^{10}$ M^{-1} s^{-1} in the absence of general acids. The rate of formation of the peroxo complex is independent of pH but is increased by general acids. This apparent general-acid catalysis is thought to arise from a combination of specific-acid and general-base catalysis. In the absence of general acids $k_6 \approx 350$ M^{-1} s^{-1}. The pH dependence of the formation constant is due to the $1/[H^+]$ dependence of the dissociation rate. Fe-EDTA is demonstrated to be a catalyst of superoxide dismutation, and the above reactions account quantitatively for the observed catalysis. It is also shown that kinetic parameters derived from steady-state analyses of superoxide decay curves can be related to the individually determined rate constants.

Superoxide is formed to a small extent in the normal functioning of aerobic organisms, and during the past several years there has been much discussion of its role in biology.[1a-j,2a-d] However, extensive studies[3a-c] of the chemistry of this species have not as yet revealed how superoxide may affect biological systems. Proponents of the view that superoxide is an important mediator of oxygen poisoning[4] have argued that superoxide and hydrogen peroxide react with trace metal ions to form reactive hydroxyl radicals.[2a,d] In spite of certain shortcomings,[1f,2c] this concept deserves careful chemical study. The purpose of this work is to explore some of the reactions of oxygen, hydrogen peroxide, and superoxide with iron complexes of ethylenediaminetetraacetic acid (EDTA).

In aqueous solution superoxide is unstable toward hydrogen peroxide and dioxygen and dismutes via reaction 1. The

$$2O_2^- + 2H^+ \rightarrow H_2O_2 + O_2 \quad (1)$$

mechanism of this process has been studied in great detail and is known to consist of two electron-transfer reactions (eq 2 and 3) and the ionization of HO_2 ($pK_a = 4.69$).[5a,b] Thus the rate of

$$2HO_2 \rightarrow H_2O_2 + O_2 \quad k_2 = 8.6 \times 10^5\ M^{-1}\ s^{-1} \quad (2)$$

$$O_2^- + HO_2 \rightarrow HO_2^- + O_2 \quad k_3 = 1 \times 10^8\ M^{-1}\ s^{-1} \quad (3)$$

reaction 1 is independent of pH below 2, increases to a maximum at the pK_a, and decreases tenfold for each pH unit increase above the pK_a.

† NSF Predoctoral Fellow. Present address: The Research Laboratories, Eastman Kodak, Rochester, New York.

Superoxide dismutation is catalyzed by various complexes of Cu, Fe, and Mn ions including a group of metalloproteins termed superoxide dismutases. Catalysis appears to require redox cycling,

(1) (a) Yamazaki, I.; Piette, L. H. *Biochim. Biophys. Acta* **1963**, *77*, 47-63. (b) Fridovich, I. *Acc. Chem. Res.* **1972**, *5*, 327-326. (c) Fridovich, I. In "Advances in Enzymology"; Meister, A., Ed.; Wiley: New York, 1974; Vol. 41, pp 35-97. (d) Bors, W.; Saran, M.; Lengfelder, E.; Spottl, R.; Michel, C. *Curr. Top. Radiat. Res. Q.* **1974**, *9*, 247-309. (e) Halliwell, B. *Cell Biology Int. Rep.* **1978**, *2*, 113-128. (f) Fee, J. A. In "Metal Ion Activation of Dioxygen"; Spiro, T. G., Ed.; Wiley: New Ork, 1980; pp 209-237. (g) Michelson, A. M., McCord, J. M., Fridovich, I., Eds. "Superoxide and Superoxide Dismutases"; Academic Press: London, 1977. (h) Fridovich, I. *Science (Washington, D.C.)* **1978**, *201*, 875-880. (i) Bannister, J. V., Hill, H. A. O., Eds. "Chemical and Biochemical Aspects of Superoxide and Superoxide Dismutase"; Elsevier/North Holland: Amsterdam, 1980. (j) Bannister, W. H., Bannister, J. V., Eds. "Biological and Clinical Aspects of Superoxide and Superoxide Dismutase"; Elsevier/North Holland: Amsterdam, 1980.

(2) (a) Fridovich, I. In "Oxygen and Oxy-Radicals in Chemistry and Biology"; Rodgers, M. A. J., Powers, E. L., Eds.; Academic Press: New York, 1981; pp 197-204, 221-239. (b) Fee, J. A. In "Oxygen and Oxy-Radicals in Chemistry and Biology"; Rodgers, M. A. J., Powers, E. L., Eds.; Academic Press: New York, 1981; pp 205-221, 221-239. (c) Fee, J. A. *Trends Biochem. Sci. (Pers. Ed.)* **1982**, *7*, 84-86. (d) Halliwell, B. *Ibid.* **1982**, *7*, 270-272.

(3) See the following review articles: (a) Fee, J. A.; Valentine, J. S. In "Superoxide and Superoxide Dismutases"; Michelson, A. M., McCord, J. M., Fridovich, I., Eds.; Academic Press: London, 1977; pp 19-60. (b) Lee-Ruff, E. *Chem. Soc. Rev.* **1977**, *6*, 195-214. (c) Sawyer, D. T.; Valentine, J. S. *Acc. Chem. Res.* **1981**, *14*, 393-400.

(4) McCord, J. M.; Keele, B. B., Jr.; Fridovich, I. *Proc. Natl. Acad. Sci. U.S.A.* **1971**, *60*, 1024-1027.

(5) (a) Bielski, B. H. J. *Photochem. Photobiol.* **1978**, *28*, 645-649. (b) Bielski, B. H. J.; Allen, A. O. *J. Phys. Chem.* **1977**, *81*, 1048-1050. See also references therein.

0002-7863/83/1505-5290$01.50/0

and a widely discussed mechanism involves cyclic reduction and reoxidation of the metal ion.

$$M^{n+} + O_2^- \rightarrow M^{(n-1)+} + O_2$$

$$M^{(n-1)+} + O_2^- + 2H^+ \rightarrow M^{n+} + H_2O_2$$

Most work has been done with Cu complexes.[6a-e] Rabani and his co-workers[7a,b] studied the extremely efficient catalysis of reaction 1 by $Cu^{2+}(aq)$ in the pH range 3.5–6.0. The reduction reaction was first order in both Cu^{2+} and superoxide and depended on the ionization state of superoxide: for HO_2 the rate constant was $\sim 1 \times 10^8$ M^{-1} s^{-1} and for O_2^- it was $\sim 8 \times 10^9$ M^{-1} s^{-1}. The reaction between Cu^+ and O_2^- occurred with $k \approx 10^{10}$ M^{-1} s^{-1}. As the coordination positions of Cu^{2+} become increasingly occupied by ligands other than H_2O, the rate of reduction by O_2^- decreases.[7b] Weinstein and Bielski[8] carefully examined the copper(II)–histidine system and demonstrated that only one of six distinct complexes present in the equilibrium mixture $(Cu(His)_2H)^{3+}$ possessed superoxide dismutase activity. The overall rate constant for this catalyst was 3.4×10^8 M^{-1} s^{-1}. Cupric complexes in which all coordination positions are blocked by chelates such as EDTA do not catalyze reaction 1.[9] Detailed studies of the Cu-containing bovine superoxide dismutase by Fielden and his co-workers[10a,b] have shown that catalysis of reaction 1 is diffusion controlled, and both reduction and reoxidation have rate constants near 2×10^9 M^{-1} s^{-1} (cf. also ref 10c).

Relatively little work has been done with small complexes of Mn. The aquo ion complex $Mn^{2+}(aq)$[11a,b] and the manganese(2+)–quinolinol complex[12] have been claimed to have superoxide dismutase activity, although mechanistic details are lacking. Bielski and Chan[13] have shown that $Mn^{2+}(aq)$ reacts with O_2^- to form a relatively stable complex, but it is not known whether this species can be reduced by O_2^- to effect a catalysis of reaction 1. Mn^{2+}–EDTA lacks catalytic activity but forms a relatively stable complex with O_2^- which is not reduced by O_2^-.[14] Pulse radiolysis studies of the Mn-containing superoxide dismutases[15a,b] have revealed a complicated catalytic process during which the protein is converted by reaction with O_2^- from an efficient catalytic form to a less efficient one. The overall catalytic rate constant was found to be 5.6×10^8 M^{-1} s^{-1}; details of the individual reactions are lacking (see also ref 15c).

Limited studies[16a-d] suggest small coordination complexes of Fe can also possess superoxide dismutase activity. Pulse radiolysis studies of the Fe-containing superoxide dismutases indicated a catalytic rate constant of 3×10^8 M^{-1} s^{-1} and suggested the intermediacy of $Fe-O_2^-$ complexes with the *E. coli* protein.[17a,b]

Chart I

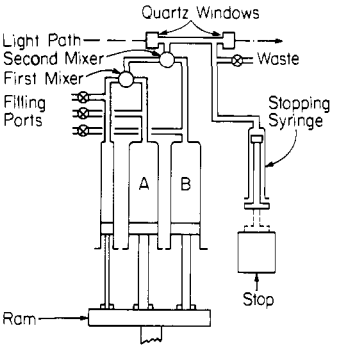

In this work we have taken advantage of the relatively slow reactions of Fe–EDTA with O_2^- to examine the mechanism by which this complex catalyzes superoxide dismutation. Previous studies showed that O_2^- would reduce Fe^{3+}–EDTA[18] (reaction 4) and participate in an oxidative addition reaction with Fe^{2+}–EDTA to form a peroxo complex[18,19] (reaction 5). This complex, first described by Cheng and Lott in 1956[20] and characterized in considerable detail by others,[21-24] also results from the reversible reaction of Fe^{3+}–EDTA with H_2O_2 (reaction 6). The direct observation of the peroxo complex during superoxide dismutation[19] suggested that reactions 4–6 (neglecting protons) combine to form a catalytic cycle. In this paper we examine each step of this cycle.

$$Fe^{3+}\text{–EDTA} + O_2^- \rightarrow Fe^{2+}\text{–EDTA} + O_2 \quad (4)$$

$$Fe^{2+}\text{–EDTA} + O_2^- \rightarrow Fe^{3+}\text{–EDTA–}O_2^{2-} \quad (5)$$

$$Fe^{3+}\text{–EDTA} + H_2O_2 \rightleftharpoons Fe^{3+}\text{–EDTA–}O_2^{2-} + 2H^+ \quad (6)$$

Materials and Methods

Solutions of O_2^- in Me_2SO were prepared by triturating 0.2 g of KO_2 (Alfa), 0.2 g of 18-crown-6 (PCR, Gainesville), and 5 mL of Me_2SO (Aldrich spectrophotometric grade) for ten minutes in a nitrogen atmosphere. Undissolved material was allowed to settle for an hour, and the slightly yellow solution decanted, assayed by means of an oxygen electrode,[25,26] and diluted to the desired concentration. Stock solutions could be stored frozen at −20 °C for several months. Dilute solutions stored at room temperature decayed about 10%/day.

Fe^{3+}–EDTA (Sigma) was used as received. Fe^{2+}–EDTA was prepared by dissolving $Fe(ClO_4)_2$ (G. Frederick Smith) and a twofold excess of Na_4EDTA in a salt solution (as needed) under inert atmosphere. The resulting pH was near 11 and any Fe^{3+} precipitated on standing. The solution was filtered and diluted anaerobically. Iron was determined as Fe^{3+}–EDTA–O_2^{2-} by using an extinction coefficient of 530 M^{-1} cm^{-1} at 520 nm.[21]

H_2O_2 (Mallinckrodt) was diluted into 1 M sodium perchlorate and determined daily by titration with potassium permanganate. Sodium perchlorate (G. Frederick Smith) was used to maintain the ionic strength at 1. Water was purified by using a Millipore Milli-Q system. All solutions contained 10^{-4} M EDTA in addition to any Fe–EDTA. All

(6) (a) Paschen, W.; Weser, U. *Biochim. Biophys. Acta* **1973**, *327*, 217–222. (b) Brigelius, R.; Spottl, R.; Bors, W.; Lengfelder, E.; Savan, M.; Weser, U. *FEBS Lett.* **1974**, *47*, 72–75. (c) Brigelius, R.; Hartmann, H.-J.; Bors, W.; Savan, M.; Lengfelder, E.; Weser, U. *Hoppe-Seyler's Z. Physiol. Chem.* **1975**, *356*, 739–745. (d) deAlvare, L. R.; Goda, K.; Kimura, T. *Biochem. Biophys. Res. Commun.* **1976**, *69*, 687–694. (e) O'Young, C.-L.; Lippard, S. J. *J. Am. Chem. Soc.* **1980**, *102*, 4920–2924.

(7) (a) Rabani, J.; Klug-Roth, D.; Lilie, J. *J. Phys. Chem.* **1973**, *77*, 1169–1175. (b) Klug-Roth, D.; Rabani, J. *J. Phys. Chem.* **1976**, *80*, 588–591.

(8) Weinstein, J.; Bielski, B. H. J. *J. Am. Chem. Soc.* **1980**, *102*, 4916–4919.

(9) Joester, K. E.; Jung, G.; Weber, U.; Weser, U. *FEBS Lett.* **1972**, *25*, 25–28.

(10) (a) Bray, R. C.; Cockle, S. A.; Fielden, E. M.; Roberts, P. B.; Rotilio, G.; Calabrese, L. *Biochem. J.* **1974**, *139*, 43–48. (b) Fielden, E. M.; Roberts, P. B.; Bray, R. C.; Lowe, D. J.; Mautner, G. N.; Rotilio, G.; Calabrese, L. *Biochem. J.* **1974**, *139*, 49–60. (c) Klug, D.; Rabani, J.; Fridovich, I. *J. Biol. Chem.* **1972**, *247*, 4839–4842.

(11) (a) Chen, K.-L.; McCay, P. B. *Biochem. Biophys. Res. Commun.* **1972**, *48*, 1412–1418. (b) Archibald, F. S.; Fridovich, I. *J. Bacteriol.* **1981**, *145*, 442–451.

(12) Howie, J. K.; Sawyer, P. C. *J. Am. Chem. Soc.* **1978**, *98*, 6698–6700.

(13) Bielski, B. H. J.; Chan, P. C. *J. Am. Chem. Soc.* **1978**, *100*, 1920–1921.

(14) Stein, J.; Fackler, J. P., Jr.; McClune, G. J.; Fee, J. A.; Chan, L. T. *Inorg. Chem.* **1979**, *18*, 3511–3519.

(15) (a) McAdam, M. E.; Fox, R. A.; Lavelle, F.; Fielden, E. M. *Biochem. J.* **1977**, *165*, 71–79. (b) McAdam, M. E.; Lavelle, F.; Fox, R. A.; Fielden, E. M. *Biochem. J.* **1977**, *165*, 81–87. (c) Pick, M.; Rabani, J.; Yost, F.; Fridovich, I. *J. Am. Chem. Soc.* **1974**, *96*, 7329–7333.

(16) (a) Halliwell, B. *FEBS Lett.* **1975**, *56*, 34–38. (b) Pasternack, R. F.; Halliwell, B. *J. Am. Chem. Soc.* **1979**, *101*, 1026–1031. (c) Pasternack, R. F.; Skowronek, W. R., Jr. *J. Inorg. Biochem.* **1979**, *11*, 261–267. (d) Peretz, P.; Solomon, D.; Weinraub, D.; Faraggi, M. *Int. J. Radiat. Biol.* **1982** *42*, 449–456.

(17) (a) Lavelle, F.; McAdam, M. E.; Fielden, E. M.; Puget, K.; Michelson, A. M. *Biochem. J.* **1977**, *161*, 3–11. (b) Fee, J. A.; McClune, G. J.; O'Neill, P.; Fielden, E. M. *Biochem. Biophys. Res. Commun.* **1981**, *100*, 377–384.

(18) Ilan, Y.; Czapski, G. *Biochim. Biophys. Acta* **1977**, *498*, 386–394.

(19) McClune, G. J.; Fee, J. A.; McClusky, G. A.; Groves, J. T. *J. Am. Chem. Soc.* **1977**, *99*, 5220–5222.

(20) Cheng, K. L.; Lott, P. F. *Anal. Chem.* **1956**, *28*, 462–465.

(21) Ringbom, A.; Sittonen, S.; Saxon, B. *Anal. Chim. Acta* **1957**, *16*, 541–545.

(22) Orhanovic, M.; Wilkins, R. G. *Croat. Chem. Acta* **1967**, *39*, 149–154.

(23) Walling, C.; Kurz, M.; Schugar, H. F. *Inorg. Chem.* **1970**, *9*, 931–937 and references therein.

(24) Wilkins, R. G.; Yelin, R. E. *Inorg. Chem.* **1969**, *8*, 1470–1473.

(25) Valentine, J. A. In "Biochemical and Clinical Aspects of Oxygen"; Caughey, W. S., Ed.; Academic Press: New York, 1979; pp 659–675.

(26) Fee, J. A.; Hildenbrand, P. G. *FEBS Lett.* **1974**, *39*, 79–81.

other chemicals were of the highest quality commerically available and were used without further purification.

Stopped-Flow Apparatus. We have described a stopped-flow spectrophotometer capable of mixing miscible organic solvents with water in a very short time[27] and demonstrated its usefulness for examining largely aqueous solutions of O_2^-.[28] However, most kinetic measurements described herein were made with a much improved apparatus equipped with three drive syringes and two mixers (Chart I). The drive syringes (two 2.5 mL and one 0.25 mL) and the stopping syringe (0.5 mL) were obtained from Unimetrics. Stainless-steel fittings (SSI Co) and 0.040 in. i.d. tubing (Anspec Co.) were used to connect the syringes and the mixers. The first mixer, wherein one part of Me_2SO solution was combined with ten parts of aqueous dilute buffer, followed the organo–aqueous ball mixer design previously described.[27] The solution was then split into four streams and recombined for more thorough mixing, necessary when mixing organic solvents and water. The second mixer combined this solution with another ten parts of solution from the third syringe. This mixer was similar to that described by Ballou.[29] The light path was 2 cm.

System performance was tested by using the dichlorophenol–indophenol (DCPIP) and ascorbic acid reaction at pH 3, taking the dead time from the slope of a semilog plot of the absorbance during flow vs. ascorbic acid concentration.[30] Phthalate buffer (0.05 M, pH 4) was used to confirm the initial absorbance of the acid form of DCPIP in a spectrophotometer. The sodium salt of DCPIP was dissolved in Me_2SO and placed in the small syringe. Ascorbate solutions were added either in the second mixer or in both mixers. The dead time was ~5 ms from the upstream mixer and ~2 ms from the downstream mixer. Complete mixing was observed for all rates less than 600 s^{-1}. There were no optical artifacts due to the organic solvent. Data were collected and manipulated on a Nova II minicomputer using software and an interface built by On Line Instrument Systems (Athens, Ga.).

Mixing Order. In experiments on Fe^{3+}–EDTA–O_2^{2-} decay, an O_2^- solution in Me_2SO was placed in the small syringe and mixed with Fe^{2+}–EDTA in 1 M $NaClO_4$ at pH ~10.5 (unbuffered) in syringe A (Chart I). At this pH, virtually no decomposition of Fe^{3+}–EDTA–O_2^{2-} occurred by the time the solution reached the second mixer and an appropriate buffer in syringe B was added. For Fe^{3+}–EDTA–O_2^{2-} formation via reaction 5, O_2^- in Me_2SO was mixed first with 1 M sodium perchlorate in syringe A buffered to pH 10 by 100 μM EDTA and then with Fe^{2+}–EDTA. For study of the rate of reaction 6, H_2O_2 solutions from syringe A were mixed with Me_2SO from the small syringe in the first mixer and then with Fe^{3+}–EDTA from syringe B in the second mixer. With the higher pH buffers, the natural acidity of the H_2O_2 and any dissolved CO_2 were neutralized by including an appropriate amount of tetrabutylammonium hydroxide in the Me_2SO. The O_2^- decay experiments had O_2^- in Me_2SO in the small syringe and buffer in each of the large syringes with Fe^{3+}–EDTA (if present) added at the second mixer. The extinction coefficient of O_2^- at 285 nm was taken to be 700 M^{-1} cm^{-1}.[5a]

Data Analysis. For computer fitting, O_2^- decay data consisted of 200 points in each of two time ranges. The decay velocity was calculated at each point by least-squares fitting the three points on either side to a straight line (for the three points at each end of a block, the first or last seven points were fitted to a quadratic). Data taken in buffer with no added Fe^{3+}–EDTA conformed to the equation

$$-d[O_2^-]/dt = k_i[O_2^-] + 2k_1[O_2^-]^2$$

where k_1 is the apparent second-order self-dismutation rate constant and k_i describes the relatively minor effect of ubiquitous trace metal impurities. This equation is linear in the unknown rate constants and is easily solved by standard least-squares techniques.[31] These rate constants are not altered by the addition of catalyst, and they were used to correct the velocity observed in the presence of catalyst to reflect only the reaction component due to the catalyst. The expression involving saturation effects (see Discussion) is nonlinear and required an iterative solution.

Other Apparatus and Methods. The pH was measured with a Radiometer GK2321C combination electrode. The use of concentrated $NaClO_4$ solutions and 4% v/v Me_2SO produced a sizeable downward shift in the pH reading starting after 30 s and stabilizing after several minutes, apparently due to junction potential effects.[32a,b] After this time, the system was quite stable and reproducible; all pH values were measured in this manner. The size of the offset was −0.6 pH unit as determined from initial and final readings. This was checked by titrating standardized dilute acid with dilute base, so that $[H^+]$ was known at each point and hence pH. The observed titration curve was shifted downward 0.6 pH unit relative to the calculated curve throughout the titration. Therefore 0.6 pH unit has been added to the direct readings of all apparent pH values reported here. The apparent pK_a values of the buffers was determined by titration and are given in the legend to Figure 10. The precision of all pH measurements was estimated to be ±0.03, while the absolute accuracy should be ±0.1 pH unit. Careful attention was paid to pH control in the kinetic studies. Thus, the pH was measured before and after reaction, and buffer and reactant concentrations were adjusted so that the pH did not change by more than ±0.03 units.

Potentiometric Titrations. Acid–base titrations were performed under Ar by using a Radiometer GK2401B electrode and PHM63 meter at room temperature. Carbonate-free 0.1 N NaOH was prepared anaerobically and standardized against hydrogen potassium phthalate. Fe^{3+}–EDTA was dissolved in 0.1 M KCl to a concentration near 50 mM. A portion of this Fe^{3+}–EDTA solution was reduced with H_2 by using a palladium-on-carbon catalyst while the pH was maintained at 5 with standardized base. These stock solutions were then appropriately diluted into 0.1 M KCl containing 0.1 mM EDTA (added to avoid Fe^{3+} precipitation at high pH). Several titrations without added iron were averaged to prepare a titration curve of the diluent solution. Using this curve, the difference in hydroxide needed to reach a given pH in the presence and absence of Fe–EDTA could be determined, and this gave the quantity of OH^- bound per iron. Similar titrations were carried out on Fe^{3+}–EDTA in 1 M $NaClO_4$ by using the Radiometer GK2321C electrode.

Formation Constant of the Peroxo Complex. All static binding studies were performed on a Perkin-Elmer Model 320 spectrophotometer equipped with a thermostated cell holder. In order to minimize formation of the μ-oxo dimer of Fe^{3+}–EDTA,[24,33,34] all studies were conducted with less than 100 μM Fe^{3+}–EDTA. Measurements on the dissociation constant of Fe^{3+}–EDTA–O_2^{2-} followed the absorbance at 520 nm in a 4-cm cell. All other static measurements used 1-cm cells. Spectral studies in the UV region were not carried below 240 nm due to the absorbance of the 4% Me_2SO present. The carbonate binding constant was determined by using difference spectroscopy by titration of a constant concentration of Fe^{3+}–EDTA with carbonate buffer.

Results

Ferric EDTA Complexes. Ferric EDTA is heptacoordinate in the crystalline state[35] having six atoms donated by EDTA and one by a water molecule. Because nucleophilic ligands have been shown to associate with this complex, presumably by replacing the water molecule,[36] and these would probably alter the oxidation–reduction properties, we have examined the optical absorption spectrum of Fe^{3+}–EDTA in the buffer systems used in this study. Chloride, perchlorate, Taps ([tris(hydroxymethyl)methyl]-aminopropane sulfonic acid), Caps (cyclohexylaminopropanesulfonic acid), Hepes (*N*-(2-hydroxyethyl)piperazine-*N*′-2-ethanesulfonic acid), Tricine (*N*-tris(hydroxymethyl)methylglycine), glycine, and glycylglycine were found not to alter the near ultraviolet optical spectrum of Fe^{3+}–EDTA at the concentrations used in this work. Carbonate was found to bind to Fe^{3+}–EDTA (see below).

Previous studies by Schwarzenbach and Heller[37] and Gustafson and Martell[33] revealed the presence of a dissociable proton on Fe^{3+}–EDTA with $pK_a \approx 7.6$, and this was interpreted as being due to the hydrolysis of a bound water molecule

$$Fe^{3+}\text{–EDTA–}OH_2 + OH^- \rightleftharpoons Fe^{3+}\text{–EDTA–}OH^- + H_2O$$

The former authors also claimed to have observed the addition of OH^- to the monohydroxy complex with $pK_a \approx 9.6$

$$Fe^{3+}\text{–EDTA–}OH^- + OH^- \rightleftharpoons Fe^{3+}\text{–EDTA–}(OH^-)_2$$

(27) McClune, G. J.; Fee, J. A. *Biophys. J.* **1978**, *24*, 65–69.
(28) McClune, G. J.; Fee, J. A. *FEBS Lett.* **1976**, *67*, 294–298.
(29) Ballou, D. P. Ph.D. Dissertation, The University of Michigan, 1971. Available from University Microfilms, Ann Arbor, MI.
(30) Naktani, H.; Hiromi, K. *J. Biochem.* **1980**, *87*, 1805–1810.
(31) Bevinston, P. R. "Data Reduction and Error Analysis for the Physical Sciences"; McGraw-Hill: New York, 1969.
(32) (a) Dole, M. "The Glass Electrode"; Wiley: New York, 1941. (b) Illingworth, J. A. *Biochem. J.* **1981**, *195*, 259–262.
(33) Gustafson, R. L.; Martell, A. E. *J. Phys. Chem.* **1963**, *67*, 576–582.
(34) Schugar, H. J.; Rossman, G. R.; Bavraclough, C. G.; Gray, H. B. *J. Am. Chem. Soc.* **1972**, *94*, 2683–2690.
(35) Lind, M. D.; Hamor, M. J.; Hamor, T. A.; Hoard, J. L. *Inorg. Chem.* **1964**, *3*, 34–43.
(36) Philip, C. V.; Brooks, D. W. *Inorg. Chem.* **1974**, *13*, 384–386.
(37) Schwarzenbach, G.; Heller, J. *Helv. Chim. Acta* **1951**, *34*, 576–591.

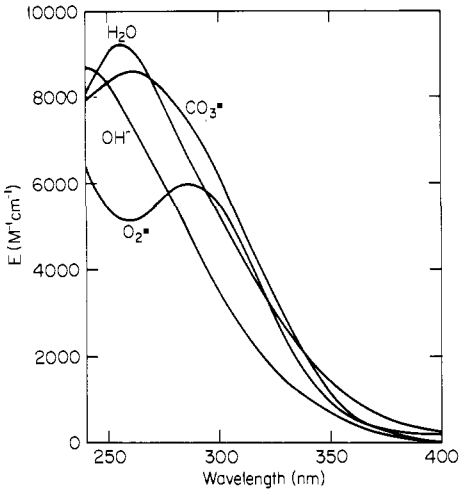

Figure 1. Near-ultraviolet absorption spectra of Fe^{3+}–EDTA complexes encountered in this study. Symbols indicate the presumed seventh ligand (see text). The CO_3^{2-} spectrum was obtained by extrapolating to infinite CO_3^{2-} concentration. Conditions: 84×10^{-6} M Fe-EDTA, 1×10^{-4} M EDTA, 5% Me_2SO, 1 M $NaClO_4$, 25 °C.

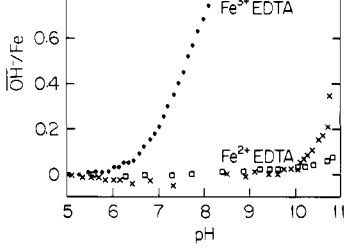

Figure 2. Potentiometric titration of Fe^{2+}- and Fe^{3+}–EDTA with KOH. Results are presented as equivalents of OH^- consumed per iron as a function of pH on raising the pH above 5: ●, 1.66×10^{-4} M Fe^{3+}–EDTA; ×, 1.66×10^{-4} M Fe^{2+}–EDTA; □, 1.61×10^{-3} M Fe^{2+}–EDTA. The solutions contained 0.1 M KCl and 10^{-4} M EDTA and were maintained under wet, O_2-free Ar at 25 °C.

The optical absorption spectrum of Fe^{3+}–EDTA–OH_2 is shown in Figure 1 for which we find $\lambda_{max} = 256$ nm and $\epsilon = 9290$ M^{-1} cm^{-1}, values in close agreement with the literature.[38] As the pH of a dilute solution of Fe^{3+}–EDTA–H_2O was raised from 6 to 10.7, the spectrum changed to that labeled *OH*⁻ in Figure 1 (λ_{max} = 240 nm, $\epsilon = 8800$ M^{-1} cm^{-1}). The absorbance changes yielded a pK_a of 7.6, and an isosbestic point at 245 nm was maintained throughout the titration. Therefore, if an additional hydroxide is binding to the metal, it does not alter the absorption spectrum. Since this seemed unlikely, we carried out a potentiometric titration the results of which are shown in Figure 2. An ionization with a pK_a at 7.6 was observed, confirming the earlier work, but no further ionization was observed up to pH 11. We are led to conclude that Fe^{3+}–EDTA binds only one hydroxyl group in the pH region of stability. The data of Gustafson and Martell[33] are consistent with this conclusion as well as the remainder of our data (see also ref 39).

Carbonate forms a complex with Fe^{3+}–EDTA. This was observed by varying the concentration of carbonate and recording the optical spectrum. The difference spectrum at pH 9.6 showed an isosbestic point at 250 nm and a maximum positive difference at 295 nm. Absorbance changes corresponded to simple binding of carbonate (assumed to be a stronger ligand than bicarbonate) and yielded a dissociation constant of 0.23 M. The spectrum (extrapolated to infinite carbonate concentration, labeled CO_3^{2-} in Figure 1) had $\lambda_{max} = 260$ nm and $\epsilon = 8700$ M^{-1} cm^{-1}.[40] Thus carbonate is a noninnocent buffer and was found to interfere with formation of the peroxo complex (data not shown).

Finally, the UV spectrum of the peroxo complex, labeled O_2^{2-}, is shown in Figure 1 ($\lambda_{max} = 287$ nm, $\epsilon = 6100$ M^{-1} cm^{-1}). The spectrum shown has been corrected for absorbance of excess H_2O_2 and corresponds to 97% formation of the complex. This agrees closely with that reported by Ilan and Czapski[18] for the product of the reaction between O_2^- and Fe^{2+}–EDTA, and previous work[19] has shown the identity of the visible spectrum of Fe^{3+}–EDTA–O_2^{2-} formed by reactions 5 and 6 ($\lambda_{max} = 520$ nm, $\epsilon = 530$ M^{-1} cm^{-1}).

Ferrous EDTA Complexes. We have assumed that Fe^{2+}–EDTA has a structure similar to Fe^{3+}–EDTA. Woodruff and Margerum[41] suggested that certain oxidants are able to bind directly to the Fe of this complex, and the previous observation[19] of an oxidative addition reaction with O_2^- is consistent with this idea. Schwarzenbach and Heller[37] reported that Fe^{2+}–EDTA released one proton with $pK_a \approx 9.1$ and a second $pK_a \approx 9.6$. We have carried out a potentiometric titration of Fe^{2+}–EDTA over the pH range 5–11 under strict anaerobic conditions and failed to observe any ionizations as the data in Figure 2 illustrate. We are led to conclude that if Fe^{2+}–EDTA binds a water molecule, the latter does not hydrolyze in our experimental conditions.

Interfering Reactions 7, 8, and 9. Several ancillary reactions that might interfere in the study of the catalytic scheme are eq 7–9. While these reactions are important in themselves, our

$$Fe^{2+}\text{–EDTA} + O_2 \rightarrow Fe^{3+}\text{–EDTA} + O_2^- \quad (7)$$

$$Fe^{2+}\text{–EDTA} + H_2O_2 \rightarrow Fe^{3+}\text{–EDTA} + OH\cdot \quad (8)$$

$$2Fe^{3+}\text{–EDTA–}OH^- \rightleftharpoons \text{dimer}^{24} \quad (9)$$

studies were only directed at assessing their potential interference in the catalytic cycle (reactions 4–6). Except in the presence of very high concentrations of peroxide none of these reactions significantly interfere.

The reaction of Fe^{2+}–EDTA with either O_2 or H_2O_2 was followed spectrophotometrically at 277 nm where Fe^{3+}–EDTA–OH^- and Fe^{3+}–EDTA–O_2^{2-} absorb equally (Figure 1). The rate of autoxidation was proportional to O_2 and nearly proportional to Fe^{2+}–EDTA concentration. Under pseudo-first-order conditions, $[O_2] \gg [Fe^{2+}\text{–EDTA}]$, the reaction was exponential except at the lower pH where some deviation was observed suggesting additional reactions. The rate constant showed no trend between pH 7.6 and pH 10.7 and had an average velocity constant of $(6 \pm 1) \times 10^2$ M^{-1} s^{-1}. Similarly, the oxidation of Fe^{2+}–EDTA by H_2O_2 was first order in both H_2O_2 and Fe^{2+}–EDTA concentrations (examined in the concentration range $[Fe^{2+}\text{–EDTA}] = 10$–$40$ μM) and was independent of pH between 8 and 10 with a velocity constant of $(2 \pm 1) \times 10^4$ M^{-1} s^{-1}. Similar values were reported by Borggaard et al.[42] These data are consistent with the previous report[19] that substoichiometric concentrations of Fe–EDTA salts do not alter the stoichiometry of reaction 1.

The dimerization of Fe^{3+}–EDTA occurs maximally above pH 8[33] and forms to a significant extent only when the total concentration is high (11% when $Fe_{tot} = 1 \times 10^{-4}$ M). The dimer is unreactive toward peroxide and must dissociate to form the peroxo complex. Fe^{2+}–EDTA is assumed not to dimerize.

The Catalytic Process. Oxidative Addition. The stoichiometry of the reaction between Fe^{2+}–EDTA with O_2^- was determined by measuring the absorbance at 520 nm within a few milliseconds after mixing known amounts of O_2^- and Fe^{2+}–EDTA. The results

(38) Schugar, H. J.; Hubbard, A. T.; Anson, F. C.; Gray, H. B. *J. Am. Chem. Soc.* **1969**, *91*, 71–77.
(39) Mader, P. M. *J. Am. Chem. Soc.* **1960**, *82*, 2956–2961.

(40) Phosphate, presumably HPO_4^{2-}, was found to produce similar perturbations in the optical spectrum of Fe^{3+}–EDTA. At pH 8.0 in 0.1 M Hepps (*N*-2-hydroxyethylpiperazine-*N*′-propanesulfonic acid) buffer, the association constant was estimated at ~ 5 M^{-1}. The following at 0.1 M caused no spectral changes: Cl^-, $HCOO^-$, oxalate, or phenol. Fluoride gave small changes at 0.7 M, and azide at 0.2 M caused a new band to develop near 400 nm. Thus, "hard" anions associate only weakly with Fe^{3+}–EDTA.
(41) Woodruff, W. H.; Margerum, D. W. *Inorg. Chem.* **1974**, *13*, 2578–2585.
(42) Borggaard, O. K.; Farver, O.; Andersen, V. S. *Acta Chem. Scand.* **1971**, *45*, 3541–3543.

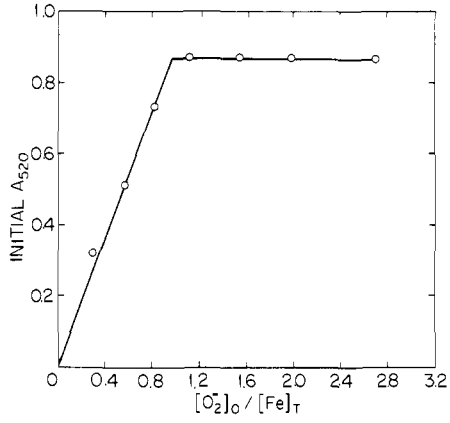

Figure 3. Stopped-flow spectrophotometric titration of Fe^{2+}–EDTA with O_2^-. Increasing concentrations of O_2^- in Me_2SO were mixed with a constant concentration of Fe^{2+}–EDTA, and the absorbance at 520 nm was recorded immediately after stop of flow. Conditions: Fe^{2+}–EDTA, 1×10^{-3} M; EDTA, 1×10^{-2} M; carbonate buffer, 0.2 M, pH 10.6; light path = 2 cm.

shown in Figure 3 demonstrate the 1:1 stoichiometry of the reaction and that the presence of excess O_2^- does not lead to a decrease in the amount of peroxo complex.

Formation of the complex in this manner is rapid, approaching the limits of the stopped-flow technique. Ilan and Czapski[18] measured the rate constant at low ionic strength over the pH range 9–11.8 using a pulse radiolysis technique. A value of $(2 \pm 0.3) \times 10^6$ M^{-1} s^{-1} was observed at pH 9 and 10, and this increased about 50% at pH 11.8. McClune[43] measured this rate constant at pH 10 and $I = 0.15$ using a competition with the bovine Cu–superoxide dismutase and obtained a value of 4×10^6 M^{-1} s^{-1}. The stopped-flow apparatus allowed direct observation of Fe^{3+}–EDTA–O_2^- formation from 10 μM each Fe^{2+}–EDTA and O_2^- and gave a value of $\sim 8 \times 10^6$ M^{-1} s^{-1} at pH 10.4, $I = 1$, and $T = 25$ °C. Thus, this reaction is largely independent of pH, and the variation in rate with ionic strength is consistent with the net negative charge on both reactants.[44]

Reduction. Because reaction 4 is much slower than reaction 5 at pH >9, we could observe formation of Fe^{3+}–EDTA–O_2^{2-} on mixing Fe^{3+}–EDTA and O_2^- in the stopped-flow apparatus and thus measure the rate of reaction 4 by monitoring absorbance changes at 520 nm. An exemplary kinetic trace and its analysis is shown in Figure 4. At constant pH this reaction was not affected by buffer concentration or type. Our data, taken above pH 9.5, are summarized in Figure 5 and show that the rate is proportional to $[H^+]$. Ilan and Czapski[18] and Butler and Halliwell[45] studied the kinetics of this reaction at pH <9 by using pulse radiolysis, and their data are also assembled in Figure 5. Our high pH data clearly establish the $1/[H^+]$ dependence of k_5, and these extrapolate to within a factor of ~ 2 of the datum of Ilan and Czapski[18] at pH 8 and to within a factor of ~ 4 of the data of Butler and Halliwell.[45] These small discrepancies in extrapolated values undoubtedly arise from systematic differences in experimental protocol, and we suggest that the information from the three sets of data is complementary. The solid line is calculated under the assumption that Fe^{3+}–EDTA–H_2O reacts with O_2^- with a velocity constant of 2×10^6 M^{-1} s^{-1} and that Fe^{3+}–EDTA–OH^- is unreactive. The dashed lines are associated with data taken at different ionic strengths and show that the reaction velocity increases with high ionic strength. This is consistent with the interaction of like charged species. Below pH 6.5 the reaction rate increases, suggesting the onset of other processes.

Dissociation of the Peroxo Complex. The rapidity of the oxidative addition process allowed a simple direct determination of

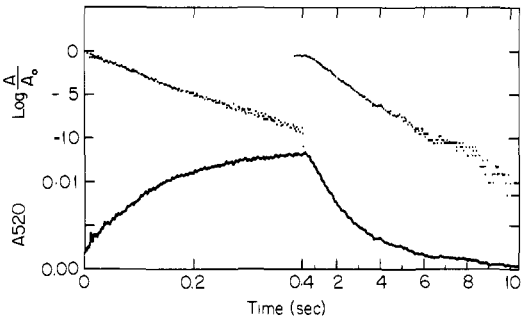

Figure 4. Demonstration of the kinetics of Fe^{3+}–EDTA reduction by O_2^- by observing formation of the peroxo complex. After mixing, the final concentrations were Fe^{3+}–EDTA = 2×10^{-4} M and O_2^- = 4×10^{-5} M. The initial increase in absorbance is due to reduction of Fe^{3+}–EDTA by O_2^- followed by rapid reaction of Fe^{2+}–EDTA with O_2^- to form the peroxo complex. The decrease in absorbance is due to the slower decay of the peroxo complex to Fe^{3+}–EDTA and H_2O_2. A logarithmic plot of A_{520}/A^0_{520} is shown in the upper right. This indicates $A^0_{520} = 0.014$ and k_{-6}(app) = 0.4 s^{-1}. This curve was extrapolated into the shorter time domain, during which reduction is occurring, and that data corrected for the small amount of peroxo complex decay which occurred during this time. The corrected data were then plotted in log format, indicated in the upper left, and correspond to an amplitude of 0.0135 and k(obsd) = $2k_4[Fe^{3+}\text{–EDTA}]_{tot} = 4.5$ s^{-1} ($k_4 = 1.13 \times 10^4$ M^{-1} s^{-1}). Conditions: 25 °C, 0.2 M Caps buffer, pH 10.4, λ = 520 nm, path = 2 cm. This procedure was used to obtain the rate constants presented in Figure 5.

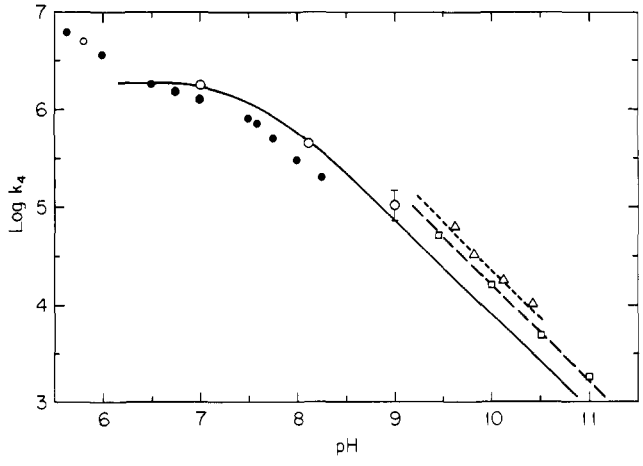

Figure 5. Rate of reduction of Fe^{3+}–EDTA by O_2^-. Open circles show the data of Ilan and Czapski[18] while closed circles show the data of Butler and Halliwell[45] taken at 0.1 M ionic strength, squares show data taken by McClune[43] at 0.15 M ionic strength, and crosses give data taken at an ionic strength of 1 M, all near 25 °C. The solid line shows the expected behavior assuming that reduction of the Fe^{3+}–EDTA–H_2O by O_2^- occurs at a rate of 2×10^6 M^{-1} s^{-1} and that Fe^{3+}–EDTA–OH^- (pK_a = 7.6) is unreactive. Dashed lines of unit slope connect data taken at higher ionic strengths.

the dissociation rate of Fe^{3+}–EDTA–O_2^{2-} (k_{-6}) using the three syringe stopped-flow apparatus as described in Materials and Methods. Use of 100 μM (final) Fe^{3+}–EDTA–O_2^{2-} in the presence of >50 mM buffer ensured that pH control was adequate and that the back reaction was negligible below pH 10.5. Simple exponential decays were observed which provided a direct measure of k_{-6}(app).

The observed rate depended strongly on the buffer concentration, and increased as the pH was lowered. Suspecting some form of general-acid catalysis, we plotted the observed rate as a function of the concentration of the acid form of the buffer. If the reaction proceeded only by general-acid catalysis, the data for a given buffer at various pH values should conform to a straight line intersecting the origin. However the previous data of Orhanovic and Wilkins[22] on the formation rate of Fe^{3+}–EDTA–O_2^{2-} in the absence of buffer showed no dependence on pH. The observed equilibrium constant is proportional to $1/[H^+]$,[21-23] which would imply a direct dependence of the decay rate on $[H^+]$. Thus,

(43) McClune, G. J. Ph.D. Dissertation, The University of Michigan, 1979. Available from University Microfilms, Ann Arbor, MI.
(44) Frost, A. A.; Pearson, R. G. "Kinetics and Mechanism"; Wiley: New York, 1961.
(45) Butler, J.; Halliwell, B. *Arch. Biochem. Biophys.* **1982**, *218*, 174–178.

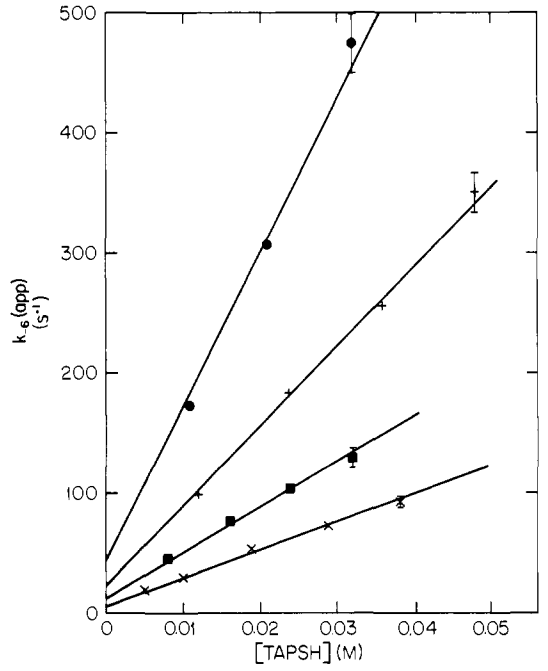

Figure 6. Rate of decay of Fe^{3+}–EDTA–O_2^{2-} in Taps buffer. [Tapsh] is the concentration of the acidic form of Taps (pK_a = 8.3) present at each dilution of the indicated pH buffer. Fe^{3+}–EDTA–O_2^{2-} was 10^{-4} M initially, at 25 °C and I = 1 M. The error bars on the highest concentration points represents the standard deviation of the mean of ten shots, about 5% of the rate, k_{-6}, while the slope gives the apparent buffer-catalyzed rate k_{-6}(buffer). ●, pH 8.06; +, pH 8.39; ■, pH 8.68; ×, pH 8.96.

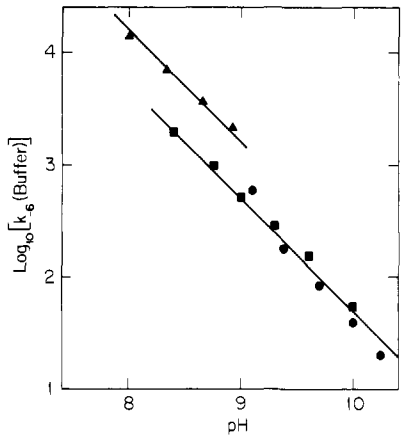

Figure 7. pH dependence of the apparent buffer-catalyzed decay rate. k_{-6}(buffer) was taken from the slope of plots similar to Figure 4. The solid lines indicate the effect of a direct dependence of k_{-6}(buffer) on [H^+]. The upper line shows the data taken in Taps at 0.1 mM Fe^{3+}–EDTA–O_2^{2-} from Figure 4. The lower line refers to carbonate buffer: ●, 0.1 mM Fe^{3+}–EDTA–O_2^{2-}; ■, 1 mM Fe^{3+}–EDTA–O_2^{2-}. The offset between the two data sets indicates that carbonate is a less efficient general acid catalyst.

the decay rate law might contain a specific-acid term plus a general-acid catalysis term. In this case, plotting k_{-6}(app) as a function of general-acid concentration at several pH values should give a family of parallel lines whose intercepts are proportional to [H^+].

Data collected in Taps buffer are shown in Figure 6. The intercepts show a direct dependence on [H^+], as expected from the data of Orhanovic and Wilkins.[22] However, the lines are not parallel but show an increase in slope as the pH decreases. This is consistent with a rate law containing the *product* [HA][H^+]. The slope of a line in Figure 6 gives the apparent buffer catalysis rate constant k_{-6}(buffer) (M^{-1} s^{-1}). In Figure 7, we have plotted log k_{-6}(buffer) as a function of pH for the Taps data of Figure 6 and for data collected in carbonate buffer. Both sets of data

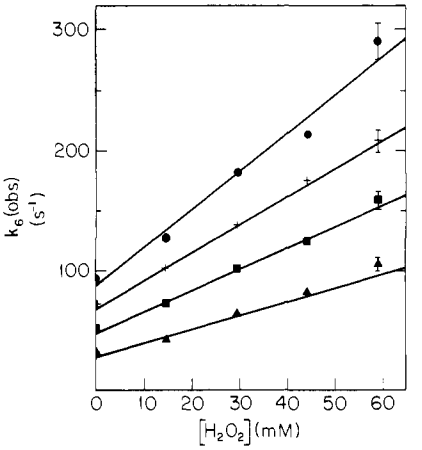

Figure 8. Rate of Fe^{3+}–EDTA–O_2^{2-} formation in pH 8.9 Taps. The symbols, ●, +, ■, and ▲ show data for total Taps concentrations of 0.19, 0.14, 0.095, and 0.048 M, respectively. The data at $[H_2O_2]$ = 0 were taken from the experiment described in Figure 6. The slopes give the apparent Fe^{3+}–EDTA–O_2^{2-} formation rate constant k_6(app). The average value of intercept/slope for these data is ~37 ± 2 M^{-1} which corresponds to the formation constant at this pH. (See Table I).

show a direct dependence on [H^+]. Therefore the complete rate law for the decay of Fe^{3+}–EDTA–O_2^{2-} to Fe^{3+}–EDTA and H_2O_2 is

$$k_{-6}(\text{app}) = k_{-6}[H^+] + k_{-6}'[H^+][HA] \qquad (10)$$

where k_{-6}' is the buffer-catalyzed decay rate constant and k_{-6} is the apparent first-order decay constant in the absence of buffer.

Since general-acid or -base catalysis must influence forward and reverse reactions equally we examined the effect of buffers on k_6.

Formation of the Peroxo Complex. Apparent first-order rate constants were obtained under the condition $[H_2O_2] >> [Fe^{3+}\text{–EDTA}]$ over a wide range of pH, buffer concentrations, and buffer species. The reaction was first order in both reactants, and apparent second-order rate constants were obtained from the slopes of k_{obsd} vs. $[H_2O_2]$ as indicated in Figure 8. Also shown in Figure 8 are the specific rates at $[H_2O_2]$ = 0 obtained from Figure 6 for the given conditions. The latter points correspond closely to the intercepts, as they should, and suggest a simple equilibrium is occurring in which the various buffers are not affecting the equilibrium. Thus, the ratio of the slope to the intercept gives a kinetic estimate of the formation constant; from the lowest to the highest buffer concentrations the data of Figure 8 yielded 40, 37, 35, and 36 M^{-1}. The measured constant at pH 8.9 was 37 M^{-1}, showing good agreement between kinetic and static measures of the formation constant (see below).

The slope of the lines if Figure 8 gave the apparent formation rate k_6(app). Expecting general-acid catalysis, we plotted k_6(app) as a function of general-acid concentration in Figure 9. From the common intercept of these lines we obtained a value of 350 M^{-1} s^{-1} for k_6 which is consistent with the value of 250 M^{-1} s^{-1}, determined by Orhanovic and Wilkins[22] in the absence of buffer. The rate law for formation of Fe^{3+}–EDTA–O_2^{2-} is thus

$$k_6(\text{app}) = k_6[H_2O_2] + k_6'[H_2O_2][HA] \qquad (11)$$

Also shown in Figure 9 are data taken in Caps buffer in the region of its pK_a (= 10.4). General-acid catalysis was again evident, although much weaker, and interfering processes were suggested by the increased intercept at high pH. This apparent complication was not studied further.

Fe^{3+}–EDTA–O_2^{2-} formation in carbonate buffer was complicated by the presence of the carbonate complex reported above. However, bicarbonate is an effective general-acid catalyst. The solid line in Figure 9 (labeled B) is drawn through points taken at low carbonate concentration. At higher concentrations, k_6(app) showed a nonlinear dependence on carbonate concentration, and the nonlinearity was influenced by pH. This behavior is shown in Figure 9 for pH 9.6 only.

Table I. Formation and Decay of the Fe-EDTA Peroxo Complex

		formation rates		decay rates		formation constant, M^{-1}		
pH	buffer	independent, M^{-1} s^{-1}	[HA] dependent M^{-2} s^{-1}	independent, s^{-1}	[HA] dependent, M^{-1} s^{-1}	static[d]	independent[e]	[HA] dependent[e]
8.00	Taps			*a*	14000			
8.35	Taps			~27	6900			
8.63	Taps	~380	66 000	20	3300			
8.91	Taps	360	71 600	10	2100	37	36	34
9.13	carbonate	*b*	*b*	6	560			
9.37	carbonate	~320[c]	31 000[c]	2.9	212			
9.70	carbonate	360[c]	30 000[c]	1.4	109	250-300[c]	260	275
9.97	carbonate	*b*	*b*	0.85	39			
10.21	carbonate	*b*	*b*	0.63	20			
9.63	Caps			*c*	~24			
10.15	Caps	385	1 340	0.6	2.1	588	640	638
10.45	Caps			0.3	1.4			
10.72	Caps	420	1 800	0.2	~1.0			
9.08	glycine			5	430			
8.80	gly-gly			*a*	19000			
8.62	tricine			14	8800			
8.13	Hepes			*a*	83000			

[a-e] Performed at 1 M ionic strength and 25 °C: *a*, difficult extrapolation to intercept; *b*, subject to carbonate interference; *c*, done in dilute carbonate buffer; *d*, measured as described in Materials and Methods; and *e*, ratios of formation to decay rate constants gly-gly = glycylglycine.

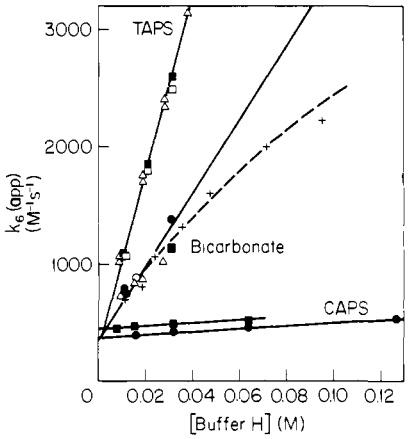

Figure 9. General-acid catalysis of Fe^{3+}–EDTA–O_2^{2-} formation. The apparent formation rate k_6(app) came from plots similar to Figure 8. [HA] is the actual concentration of the acid form of the buffer, Taps (pK_a = 8.3), carbonate (pK_a = 9.6), or Caps (pK_a = 10.4). The symbols ×, ●, +, ■, and △ refer to data taken at a pH above or below the pK_a of the buffer as follows: −0.6, −0.3, at pK_a, +0.3, and +0.6, respectively. The intercepts give the buffer independent formation constant k_6 (M^{-1} s^{-1}) and the slopes the buffer-catalyzed formation rate constant k'_6 (M^{-2} s^{-1}).

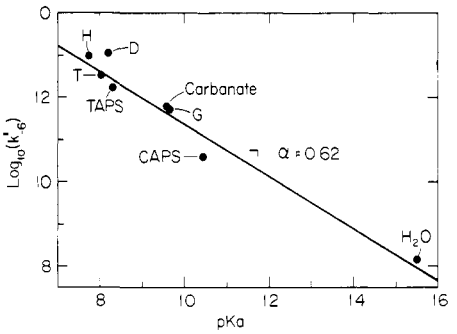

Figure 10. Brønsted plot of buffer-catalyzed formation and decay rate constants. The single letters refer to the following buffers: H, Hepes (pK_a = 7.8); T, Tricine (8.07); D, glycylglycine (8.25); G, glycine (9.7). Other pK_a values are as follows: Taps, 8.3; Caps, 10.4; carbonate, 9.7; H_2O, 15.5.

If we assume that the carbonate complex and Fe^{3+}–EDTA–OH^- are in rapid equilibrium and that the carbonate complex is unreactive with H_2O_2, we can calculate the expected reaction rate by using a carbonate dissociation constant of 0.23 M and the value for carbonate general-acid catalysis. The predicted behavior is shown by the dashed line in Figure 9. The reasonable fit to the data suggests that this simple model is correct. All rate constants are gathered in Table I.[46]

General-Acid Catalysis and Acid Strength. The relationship between the general-acid catalysis rate constants k_{-6}' and acid strength may be examined in the Brønsted plot (Figure 10). Since water is also a general acid, it is likely that it contributes to the buffer independent rates by the same mechanism as the other buffers. Therefore $k_{-6}'/52$ (52 M being the final concentration of water in the reaction mixture) is included in Figure 10. While the data are restricted to a range of two pK_a units and the structures of the acids are quite dissimilar, a linear least-squares treatment was nevertheless carried out to get some idea of the Brønsted coefficient α. If the points for H_2O and Caps are excluded, the latter of which is the most sterically hindered acid, $\alpha = 0.66 \pm 0.12$ (SD) was found. Including the Caps point gave $\alpha = 0.77$ and considering all points gave $\alpha = 0.62$. In spite of the paucity of data, the extrapolation to the H_2O point is quite reasonable and suggests that water may be serving as a general acid. A limited amount of data were obtained for the forward reaction, k_6', and these were also consistent with $\alpha \approx 0.6$. Similarly the ratios of k_{-6}' to k_6' yielded values of the formation constant of reaction 6 that were in close agreement with statically determined values (Table I).

Catalysis of Superoxide Dismutation. While reactions 4–6 constitute a catalytic cycle, catalysis will only be observed if the overall velocity of these reactions exceeds that of reaction 1. Previously published data strongly suggest that a weak catalysis by Fe–EDTA is evident in decay curves of aqueous O_2^-.[19,47] The decay curves shown in Figure 11 provide unambiguous evidence for catalysis by added Fe–EDTA. Thus, from the upper and lower curves of panel A, it can easily be shown that ~3 turnovers of the proposed cycle are required to account for the apparent catalysis.

The cycle involves breakdown of the peroxo complex, a process independent of O_2^- concentration. At sufficiently high O_2^- con-

(46) Values of k_{-6} and k_6 are given to Table I as first- and second-order constants, respectively. However, if water were acting as a general acid in the absence of buffer, the rate laws should be rewritten as $k_{-6}[H^+][H_2O] + k_{-6}'[H^+][HA]$ and k_6(app) = $k_{-6}[H_2O_2][H_2O] + k_6'[H_2O_2][HA]$, and corrected values of k_{-6} and k_6 would be gotten by dividing the given values by 52 M (the concentration of water in the reaction mixture).

(47) Bull, C.; Fee, J. A.; O'Neill, P.; Fielden, E. M. *Arch. Biochem. Biophys.* **1982**, *215*, 551–555.

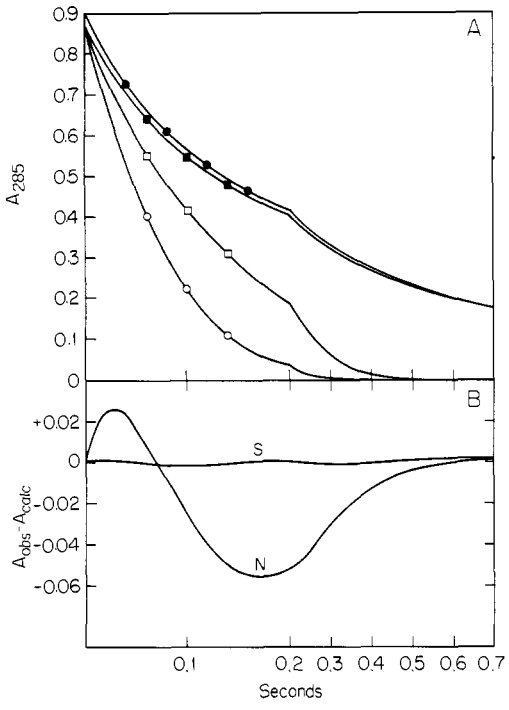

Figure 11. Catalyzed dismutation of O_2^-. The time scale changes in the middle as shown. Panel A: observed decay of the absorbance of O_2^- at 285 nm taken in glycine buffer at pH 9.1. Circles and squares refer to 0.19 and 0.048 M total glycine buffer, respectively. Closed symbols indicate no added Fe^{3+}–EDTA and open symbols indicate 42 μM Fe^{3+}–EDTA. The starting concentration of O_2^- was 630 μM. Panel B: difference between the observed data at 0.19 M buffer with 42 μM Fe–EDTA and the predictions of two models for Fe–EDTA catalysis. S represents the saturation model (reactions 4–6) while model N assumes a simple first-order dependence of the rate of catalysis on O_2^- concentration (see Discussion).

centration, this step is anticipated (see Discussion) to become rate limiting. An implication of buffer-catalyzed decomposition of Fe^{3+}–EDTA–O_2^{2-} is that when this process is controlling the overall velocity of the cycle, the catalytic efficiency of Fe–EDTA should be increased by added buffers. Experiments designed to test this prediction are shown in Figure 11. After mixing, the initial concentration of O_2^- was 640 μM and that of Fe^{3+}–EDTA was 42 μM. The disappearance of O_2^- was followed at 285 nm, near the isosbestic point of Fe^{3+}–EDTA–OH^- and Fe^{3+}–EDTA–O_2^{2-} where these species contribute approximately 30% of the total initial absorbance. The two upper curves show the dismutation of O_2^- in the absence of Fe^{3+}–EDTA at two different buffer concentrations, while the lower curves show the decay of O_2^- in these buffers in the presence of Fe–EDTA. As predicted, Fe–EDTA is clearly a better catalyst at the higher buffer concentration. The analysis of these decay curves is considered below.

Discussion

Any understanding of the mechanism of Fe–EDTA catalyzed superoxide dismutation must be based on the solution structures and dynamics of the Fe^{3+} and Fe^{2+} complexes and of the peroxo complex. The results of our potentiometric titrations of Fe^{3+}–EDTA indicate that this complex has a single bound water molecule, according to the published structure,[35] which ionizes to a hydroxyl group above pH 7.6.[48] Solutions of Fe^{3+}–EDTA have also been examined by nuclear magnetic relaxation techniques,[49a,b,50] and these studies are also consistent with the idea that the structure of Fe^{3+}–EDTA–OH_2 is the same in solution as in the crystalline state. Bloch and Navon[50] determined the rates of exchange of the water molecule, its protons, the hydroxyl group, and its proton. The residence time of the water molecule was estimated to be $(1.3 \pm 0.4) \times 10^{-6}$ s at 20 °C, and its protons were shown to exchange with the molecule as a whole. The data of these authors indicate that the hydroxyl group of Fe^{3+}–EDTA–OH^- exchanges very much slower than the H_2O of the aquated form. Indeed, all exchange may proceed through the aquo complex. No direct structural information is available for Fe^{2+}–EDTA, and it is assumed to bind a single rapidly exchanging water molecule over the entire pH range.

The structure of the peroxo complex has not been determined. However, Walling and co-workers[23] have shown that the most likely composition is Fe^{3+}–$EDTA^{4-}$–O_2^{2-} or Fe^{3+}–$EDTA^{4-}$–O_2^{2-}–H_2O to give a net charge of 3^-. They also showed that the Fe^{3+} was high-spin, $S = {}^5/_2$, and suggested that the unique spectral properties were due to $O_2^{2-} \rightarrow Fe^{3+}$ (LMCT) charge-transfer transitions. Three possible structures for this complex are

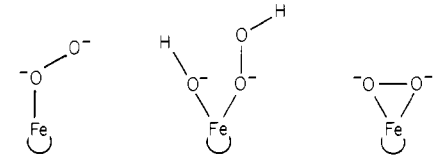

I II III

Structure I is considered unlikely because the peroxide is not expected to coordinate much more strongly than water or OH^-. Structure II, in which the elements of H_2O have been added to I, is also considered unlikely because the complex is known not to form with alkyl peroxides,[23] and no increased affinity of the peroxide for the Fe would be expected. Moreover, end-on peroxide complexes are not anticipated to generate the unusual spectral properties characteristics of the peroxo complex.[51] Walling et al.[23] also suggested that the relatively high affinity of peroxide for the iron was associated with loss of the second proton from H_2O_2.

Considerable chemical precedent now exists for cyclic peroxide structures such as III.[52,53] Recently, the structures of titanium(4+)–porphyrin cyclic peroxide compounds have been reported,[54] and an eight-coordinate diperoxymolybdenum(6+) tetra-*p*-tolylporphyrin has been described.[55] McCandlish et al.[56] have offered spectral evidence for formation of a cyclic peroxo complex resulting from the reaction of superoxide with Fe^{2+} tetraphenylporphyrin. While Mo^{6+} and Fe^{3+} have similar ionic radii[57,58] and may thus accommodate eight coordinating atoms, the Fe–EDTA complex may avoid expansion of the coordination number by dissociation of a carboxyl group. On the basis of the available information, we tentatively suggest that Fe^{3+}–EDTA–O_2^{2-} contains a cyclic peroxo arrangement of atoms (structure III).

In order to account for the dependence of the association constant of pH, the formation of the peroxo complex can be written either as

$$Fe^{3+}\text{–EDTA–}OH^- + H_2O_2 \rightleftharpoons Fe^{3+}\text{–EDTA–}O_2^{2-} + H_3O^+$$

or as

(48) The differences between our observations and those of Schwarzenbach and Heller[37] may be due to two factors: First, we included a 10^{-4} M excess of EDTA in all experiments. Second, our measurements span a period of several hours and would only detect processes occurring relatively rapidly. See also: Christensen, H.; Borggaard, O. K. *Acta Chem. Scand., Ser. A.* **1977** *A31*, 793–794.

(49) (a) Whidby, J. F.; Leyden, D. E. *Anal. Chim. Acta* **1970**, *51*, 25–30. (b) Manley, C. *Z. Angew. Phys.* **1971**, *32*, 187–190.

(50) Bloch, J.; Navon, G. *J. Inorg. Nucl. Chem.* **1980**, *42*, 693–699.

(51) Evans, M. G.; George, R.; Uri, N. *Trans. Faraday Soc.* **1949**, *45*, 230–236.

(52) Vaska, L. *Acc. Chem. Res.* **1976**, *9*, 175–183.

(53) Valentine, J. S. *Chem. Rev.* **1973**, *73*, 235–245.

(54) Guillard, R.; Latour, J.-M.; Lecomte, C.; Marchon, J.-C.; Protas, J.; Ripoll, D. *Inorg. Chem.* **1978**, *17*, 1228–1237.

(55) Cherrier, B.; Dibold, Th.; Weiss, R. *Inorg. Chim. Acta.* **1976**, *19*, 157–158.

(56) McCandlish, E.; Miksztal, A. R.; Nappa, M.; Sprenger, A. Q.; Valentine, J. S.; Stong, J. D.; Spiro, T. G. *J. Am. Chem. Soc.* **1980**, *102*, 4268–4271. See also references therein.

(57) Durant, P. J.; Durrant, B. "Introduction to Advanced Inorganic Chemistry"; Wiley: New York, 1970.

(58) Evans, M. G.; Uri, H. *Trans. Faraday Soc.* **1949**, *45*, 224–230.

$$Fe^{3+}\text{–EDTA–}OH^- + HO_2^- \rightleftharpoons Fe^{3+}\text{–EDTA–}O_2^{2-} + H_2O$$

Thermodynamic considerations alone do not distinguish between such schemes. However, the rate constant for the formation of Fe^{3+}–EDTA–O_2^{2-} is independent of pH in a region where $[HO_2^-]$ is increasing by a factor of 10 with each unit increase in pH (pK_a of H_2O_2 = 11.7[51]), while the iron complex is not ionizing. This would appear to exclude a mechanism in which HO_2^- displaces OH^- in the rate-limiting step.

The rate law for the formation of peroxo complex involves a general-acid catalyst

$$\text{rate} \propto [Fe^{3+}\text{–EDTA–}OH^-][H_2O_2][HA]$$

and implies that the transition state includes the elements of the monohydroxy Fe–EDTA complex, H_2O_2, and a general-acid catalyst, although the positions of the protons cannot be specified. The possibility that reaction occurs between HO_2^- and Fe^{3+}–EDTA–OH_2 cannot be excluded on any grounds. Indeed, the rate constant for this reaction would only need to be $\sim 3 \times 10^6$ M^{-1} s^{-1} to account for observed velocities. However, from a mechanistic view it is difficult to ascribe a reasonable role to HA in this reaction which is consistent with microscopic reversibility. Additional insight into the mechanism was obtained by studying the reverse reaction. The decay of peroxo complex follows the rate law

$$\text{rate} \propto [H^+][HA][Fe^{3+}\text{–EDTA–}O_2^{2-}]$$

suggesting that the elements of both a specific acid and a general acid are involved in the transition state.

The combined information of the two rate laws requires that the transition state include elements of the following: Fe^{3+}–EDTA, H_2O, HA, and HO_2^-. The simplest mechanism, consistent with observation, can be written if the elements of H_2O are removed by presuming the reaction to proceed via a form of Fe^{3+}–EDTA from which H_2O has dissociated. The mechanistic scheme shown in eq 12 suggests a general acid/base catalysis of peroxide ex-

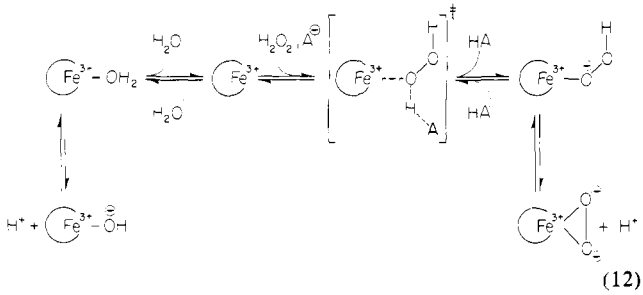

(12)

change with a nonaquated form of Fe^{3+}–EDTA. The scheme conforms to microscopic reversibility, as the velocity of the forward reaction is proportional to $[H^+][A^-][H_2O_2] \equiv [HA][H_2O_2]$ while the reverse reaction is proportional to $[H^+][HA]$ making both processes appear to be general acid catalyzed. Moreover, it accounts for the dependence of K_a on $1/[H^+]$ and, in the absence of buffers where H_2O may be acting as the general acid, predicts a pH-independent formation rate and a pH-dependent decay rate. Although a dissociative process is suggested, any form of general-base-assisted peroxide binding would be consistent with the results.

The requirement for general acid/base catalysis suggests that a basic center develops as the system approaches the transition state during breakdown and that an acidic center develops in the direction of complex formation. The Brønsted coefficient ($\alpha \approx$ 0.6–0.7, obtained from Figure 10) is a quantitative measure of the ability of weak acids to stabilize the transition state relative to their complete ionization, and α is thus a measure of the degree of proton transfer in the transition state.[59] The fact that the point for H_2O, in Figure 10, falls quite close to the extrapolated line suggests, however, that water acts as a general acid according to the proposed reaction mechanism.

We turn now to the electron-transfer reactions of the catalytic scheme. The oxidative addition of O_2^- to Fe^{2+}–EDTA to form Fe^{3+}–EDTA–O_2^{2-} requires that O_2^- bind directly to the Fe^{2+} prior to electron transfer.[19] We were not able to study this process in detail because the reaction is too rapid for our present instrumentation. However, the rate constant lies between 10^6 and 10^7 M^{-1} s^{-1}, depending on the ionic strength, and it is independent of pH in the 9–11 range. An apparently related reaction is the oxidation of Fe^{2+}–EDTA by halogens and trihalides[41] which is also rapid ($\sim 2 \times 10^6$ M^{-1} s^{-1} at pH 5 and low ionic strength) and does not depend on the overall ΔG of the reaction. These facts led Woodruff and Margerum[41] to suggest that the reaction is limited by the rate at which the oxidant coordinates to the Fe^{2+}. While there is no information available on the water-exchange rate of Fe^{2+}–EDTA, the possibility remains that these reactions are limited by the rate of exchange of the bound water.

It is important to exclude the possibility that O_2^- reduces the peroxo complex, thus inducing an alternate cycle for superoxide dismutation or a means of further reducing H_2O_2. Several results suggest this does not occur: the results of Figure 2 suggest at least that O_2^- does not rapidly reduce the complex, and Fe–EDTA does not change the stoichiometry of dismutation.[43] McClune[43] has further shown that the peroxo complex is highly resistant to reductants such as $S_2O_4^{2-}$ and BH_4^-, and Mader[39] has commented on the weak oxidative capacity of this complex. These observations tend to exclude reactions of the peroxo complex with mild reductants and are consistent with the apparently low reduction potentials of other cyclic peroxide compounds.[53,56]

Given the small discrepancies mentioned above, the combined data on the reduction of Fe^{3+}–EDTA by O_2^- (Figure 5) shows that a proton is involved in the transition state. The data between pH 7 and pH 11 suggest a reaction between Fe^{3+}–EDTA–H_2O and O_2^- rather than between Fe^{3+}–EDTA–OH^- and HO_2. The data also are consistent with an ionization at $pK_a \approx 7.6$ and suggest no reaction between O_2^- and the hydroxo complex. Below pH 7 the rate increases, which may be due to a higher concentration of HO_2 or a more reactive form of Fe^{3+}–EDTA.[60]

There are three possible mechanisms for the reductive reaction: ligand exchange followed by rapid electron transfer (S_N1 or inner sphere), addition of O_2^- with increase in coordination number followed by electron transfer, or an outer-sphere process. In the extreme case,[61] an inner-sphere reaction would be limited by the rate at which the water molecule left the complex. The reaction scheme is generally thought to involve an encounter complex

$$Fe^{3+}\text{–EDTA–}H_2O + O_2^- \rightleftharpoons [Fe^{3+}\text{–EDTA–}H_2O, O_2^- \overset{1/\tau_s}{\rightleftharpoons} Fe^{3+}\text{–EDTA–}O_2^-] \overset{\text{rapid}}{\rightarrow} Fe^{2+}\text{–EDTA–}H_2O + O_2$$

and predicts that

$$k_{obsd} = K_{os}(1/\tau_s)$$

where K_{os} is the equilibrium constant for formation of the outer-sphere complex of the reactants and τ_s is the residence lifetime of the water molecule. Using $\tau_s = 1.3 \times 10^{-6}$ s for the water molecule on Fe^{3+}–EDTA–H_2O[50] and $k_{obsd} = 2 \times 10^6$ M^{-1} s^{-1}, we calculate $K_{os} = 2.5$ M^{-1} which is quite large for two negatively charged reactants. By comparison, a value of $K_{os} \approx 0.3$ M^{-1} was estimated by using the expressions given by Brown and Sutin,[62] assuming spheres of equal radii and a separation distance of 4 Å. This is not a very large discrepancy, however, since O_2^- may interact favorably with, for example, an ion pair of Fe^{3+}–EDTA, and its affinity for the aquo complex may be increased by hydrogen bonding. Thus, an inner-sphere process cannot be ruled out. On the basis of the known ability of Fe–EDTA[63] and O_2^-[64] to ex-

(59) Bender, M. L. "Mechanisms of Homogeneous Catalysis from Protons to Proteins"; Wiley-Interscience: New York, 1971; Chapters 4 and 5.

(60) Kennard, C. H. L. *Inorg. Chim. Acta* **1967**, *1*, 347–354.
(61) Langford, C. H.; Gray, H. B. "Ligand Substitution Processes"; W. A. Benjamin: New York, 1965.
(62) Brown, G. M.; Sutin, N. *J. Am. Chem. Soc.* **1979**, *101*, 883–892.
(63) Wherland, S.; Gray, H. B. In "Biological Aspects of Inorganic Chemistry"; Addison, A. W., Cullen, W. R., Dolphin, D., James, B. R., Eds.; Wiley-Interscience: New York, 1977; pp 289–368.

Table II. Comparison of Steady-State Parameters with Reactions 4 and 6[a]

buffer, M	pH	[Fe], μM	$[O_2^-]_0$, μM	$k_{cat.}$, s^{-1}	k_{-6}, s^{-1}	K_m, μM	$k_{cat.}/K_m$, $M^{-1}\ s^{-1}$	k_4, $M^{-1}\ s^{-1}$
0.04 glycine	9.1	42	640	20	20	78	2.6×10^5	1.8×10^5
0.19 glycine	9.1	42	640	74	70	270	2.7×10^5	1.8×10^5
0.19 Caps	9.8	10	250	1.4	1.6	33	4.2×10^4	3.5×10^4
0.19 Caps	10.1	4.4	100	0.5	0.8	25	2×10^4	1.8×10^4

[a] The values of $k_{cat.}$ and K_m come from computer fits to superoxide decay curves (e.g., Figure 11). Values of k_4 are taken from the dashed line in Figure 5 while k_{-6} was determined directly. Conditions: 25 °C and I = 1 M.

change electrons with protein systems, an outer-sphere reaction is an alternative possibility. However, none of these mechanisms can be excluded by present data.[65]

Clearly reactions 4–6 constitute a catalytic cycle, and, as illustrated in Figure 11, superoxide decay is more rapid in the presence of substoichiometric amounts of Fe–EDTA and is further enhanced by the presence of buffers. It remains to be demonstrated whether the apparent catalysis of superoxide dismutation is accounted for by the operation of this cycle or by some additional processes which were overlooked.

One possible source of spurious catalysis would be Cu^{2+}, which as the aquo complex is a more efficient catalyst of superoxide dismutation than the bovine Zn/Cu enzyme. However, the EDTA complex of Cu^{2+} is devoid of activity.[9] Since our solutions contained an excess of free ligand, there is little likelihood that Cu^{2+} is responsible for the observed catalysis. A similar situation prevails with Mn^{2+} since its EDTA complex also has no catalytic activity.[14] While we cannot rule out the possibility of other, highly active metal–EDTA complexes derived from contaminating ions, such an occurrence seems unlikely.

In the remainder of this discussion we will demonstrate that reactions 4–6 can quantitatively account for the observed catalysis of superoxide dismutation. As shown below, these reactions predict an apparent saturation of the catalyst. However, let us first consider simpler, yet plausible models. The expression 13 describes a catalyst which does not saturate. If the O_2^- decay curves are

$$d[O_2^-]/dt = k_i[O_2^-] + 2k_1[O_2^-]^2 + k_{cat.}[\text{Fe–EDTA}]_{tot}[O_2^-] \quad (13)$$

adequately represented by this expression, then saturability is not characteristic of the catalyst, and the system is not behaving as predicted.

The first term represents a very weak catalytic activity in our solutions (probably Fe–EDTA at or below 2 μM) which is observed as a slight deviation from the second-order process predicted from the second term. Values of k_i and k_1 were obtained by linear least-squares analysis of data taken in the absence of added Fe–EDTA, as described in Materials and Methods. With these values as constants in expression 13, decay curves in the presence of Fe–EDTA were subjected to least-squares analysis with $k_{cat.}$ as the only floating parameter. As shown in Figure 11, the concurrence of calculated and experimental curves was not satisfactory and the residuals were quite large (Figure 11B). This tends to exclude a nonsaturable catalyst.

The rate expression shown in eq 14 includes a term which accounts for saturation of the catalyst. Here $k_{cat.}$[Fe–EDTA]

$$\frac{d[O_2^-]}{dt} = k_i[O_2^-] + 2k_1[O_2^-]^2 + \frac{k_{cat.}[\text{Fe–EDTA}][O_2^-]}{K_m + [O_2^-]} \quad (14)$$

represents the maximum velocity attributable to the catalyst and K_m corresponds to the concentration of O_2^- at half-maximal activity. If only reactions 4–6 are contributing to catalysis and the steady-state assumption is valid, then $k_{cat.}$ and K_m can be defined in terms of the individual rate constants of these reactions. Using the method of King and Altman[68] and assuming $[H_2O_2] = {}^1/_2([O_2^-]_0 - [O_2^-])$, we find

$$k_{cat.} = \frac{2k_{-6}}{(1 + k_6/2k_4)} \quad (15)$$

$$K_m = k_{-6}\frac{\left[\frac{1}{k_4} + \frac{1}{k_5} + \frac{k_6}{k_{-6}}\frac{[O_2^-]_0}{2k_4}\right]}{(1 + k_6/2k_4)} \quad (16)$$

Under the conditions of our experiments and for known values of rate constants these expressions are greatly simplified. Thus, $k_6/2k_4 < 0.05$ causing the denominators in the above expressions to approximate unity, and the last two terms in the numerator of expression 16 are negligible if the initial concentration of O_2^- is chosen such that less than 5% of the iron exists as the peroxo complex at the end of the experiment. With these approximations

$$k_{cat.} \simeq 2k_{-6} \quad (17)$$

and

$$K_m \simeq k_{-6}/k_4 \quad (18)$$

Independent values for $k_{cat.}$ and K_m can be obtained either by inserting known rate constants into expressions 17 and 18 or from nonlinear least-squares analysis of O_2^- decay curves. Since k_i and k_1 are already known precisely for the conditions of the experiment, the only floating parameters in the analysis are $k_{cat.}$ and K_m. This expression provided excellent correlation between experiment and theory as shown by the residuals in Figure 11B. Moreover, in several separate experiments spanning a range of H^+, iron, and buffer concentrations,[69] the values of these parameters calculated from independently measured rate constants were, within small limits of error, identical with those obtained from the least-squares analysis (Table II). These observations are consistent with reactions 4–6 determining the weak catalytic activity of Fe–EDTA.

The excellent representation of the experimental results by this formalism suggests that the rate-limiting step in the catalytic

(64) Simic, M. G.; Taub, I. A.; Tocci, J.; Hurwitz, P. A. *Biochem. Biophys. Res. Commun.* **1975**, *62*, 161–167.

(65) The driving force for the reaction $O_2^- + Fe^{3+}$–EDTA $H_2O \rightarrow O_2 + Fe^{2+}$–EDTA–$H_2O$ can be obtained from the potentials of the two couples (Fe^{3+}/Fe^{2+})–EDTA = 0.12 V[38] and $(O_2/O_2^-) = -0.16$V[3a] using 1 M O_2 as the standard state. From a knowledge of the forward rate and the equilibrium constant we calculate a value of ~35 $M^{-1}\ s^{-1}$ for the back reaction (reaction 7). Correcting the observed constant to a stoichiometry of 4 gives a comparable value of ~150 $M^{-1}\ s^{-1}$. The discrepancy, corresponding to as little as 35 mV in the driving force, is likely to be within the errors associated with the above potentials. Further, if we assume an outer-sphere mechanism for this reaction, we can, with knowledge of the self-exchange rate for the (Fe^{3+}/Fe^{2+})–EDTA system compute the self-exchange rate for the O_2/O_2^- complex. Thus, with use of the Marcus expression[63]

$$k_{12} = (k_{11}k_{22}Kf)^{1/2}$$

with the assumption that f = 1 and $k_{12} = 2 \times 10^6$ $M^{-1}\ s^{-1}$ and $k_{22} = 3 \times 10^4$ $M^{-1}\ s^{-1}$ for Fe–EDTA,[66] k_{11} for the O_2/O_2^- couple was found to be 2.5×10^3 $M^{-1}\ s^{-1}$. This value is quite similar to that obtained with other known outer-sphere reactions.[67a,b]

(66) Wilkins, R. G.; Yelin, R. E. *Inorg. Chem.* **1968**, *7*, 2667–2669.

(67) (a) Stanbury, D. M.; Haas, O.; Taube, H. *Inorg. Chem.* **1980**, *19*, 518–524. (b) Stanbury, D. M.; Mulac, W. A.; Sullivan, J. C.; Taube, H. *Inorg. Chem.* **1980**, *19*, 3735–3740.

(68) See: Segal, I. H. "Enzyme Kinetics"; Wiley-Interscience: New York, 1975; Chapter 9.

(69) Reactions 4–6 also predict inhibition by added peroxide due to reversible formation of the peroxo complex. However, analysis of data taken in the presence of peroxide becomes overly complicated because of increased importance of the reaction between Fe^{2+}–EDTA and H_2O_2 and subsequent, unknown reactions with the products.

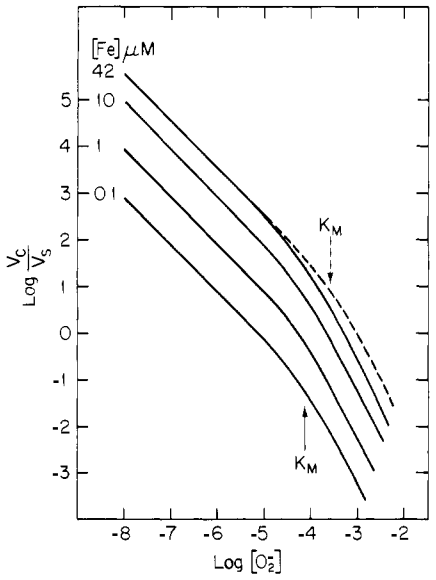

Figure 12. Plot of log (V_c/V_s) vs. log [O_2^-]. The upper curve and the dashed curve were calculated to correspond to the conditions of Figure 11. The value of k_1 was set at 3×10^3 M^{-1} s^{-1}.[5a] For the solid lines from top to bottom $k_{cat.} = 20$ s^{-1} and $K_M = 78 \times 10^{-6}$ M. The concentration of Fe–EDTA was 42, 10, 1, and 0.1 μM. The dashed line demonstrates the effect of added buffer; $k_{cat.} = 74$ s^{-1} and $K_M = 270 \times 10^{-6}$ M.

portion of superoxide decay is the breakdown of the peroxo complex, k_{-6}, when [O_2^-] $\gg$ K_M and reduction of the ferric complex when [O_2^-] $\ll$ K_M. Expression 14 also tells us that the efficiency of Fe–EDTA catalysis depends on the concentration of O_2^-. Thus, if we ignore k_i in expression 14, the velocity of O_2^- decay that is due to operation of the cycle is

$$V_c = 2k_{cat.}[\text{Fe–EDTA}][O_2^-]/(K_M + [O_2^-])$$

while that due to spontaneous dismutation is

$$V_s = 2k_1[O_2^-]^2$$

Thus considering V_c/V_s as a measure of catalytic efficiency, Figure 12 shows the dependence of V_c/V_s on the concentration of O_2^- for different concentrations of Fe–EDTA. Several conclusions are evident from these plots: (a) Fe–EDTA is a rather effective catalyst of dismutation at concentrations of $O_2^- < 10^{-6}$ M. Thus, at a concentration of 10^{-7} M Fe–EDTA and an initial concentration of $O_2^- < 10^{-6}$ M, more than 90% of the O_2^- will be catalytically dismuted. Unfortunately, below 10^{-6} M superoxide must be detected by indirect assay, and the facile electron-transfer properties of Fe–EDTA itself can interfere.[47,70] (b) When [O_2^-] $<<$ K_M, V_c/V_s reduces to $k_4[Fe]/k_1[O_2^-]$ and tells us that catalytic efficiency will be proportional to [Fe–EDTA], independent of buffer effects, and independent of pH at values above 8. The latter is due to the fact that k_4 and k_1 have the same pH dependence. (c) As [O_2^-] approaches K_M, the velocity of spontaneous dismutation rapidly increases, due to the square law dependence, the peroxo complex accumulates, and thus catalytic efficiency decreases rapidly. It is in this region where general-acid catalysis of peroxo complex breakdown increases catalytic efficiency. This is indicated by the dashed line in Figure 12. Note that at low concentrations of O_2^- buffer has no effect on V_c/V_s and this is consistent with the observation that buffers do not affect the rate of reduction, k_4.

Intimate knowledge of the mechanisms of metal ion–superoxide reactions will be required to understand superoxide dismutases. In this context, the relatively slow reactions of O_2^- with Fe–EDTA and other polyaminocarboxylatoiron complexes[43] are suitable for more detailed study. Future work should focus on discerning the mechanisms of these reactions.

Acknowledgment. This work was supported by USPHS Grant GM 21519. We are grateful to Dr. John T. Groves who first suggested that O_2^- may react with Fe^{2+}–EDTA to form the purple peroxo complex and thank him for many helpful discussions during the course of this work. We also thank Drs. H. Schngar, D. Busch, and J. Shafer for helpful discussions.

Registry No. Superoxide, 11062-77-4.

(70) The earlier claim[19] that Fe–EDTA was a catalyst of superoxide dismutation has stimulated some controversy. Diguisippi and Fridovich[71] were unable to demonstrate this catalysis using cytochrome *c* as a scavenger probe for O_2^-. These authors failed to account for the rapid reaction of Fe^{2+}–EDTA with cytochrome *c* which, as pointed out,[47] precludes any possibility of observing catalysis in their system. More recently, Butler and Halliwell[45] claimed that catalytic decay of O_2^- could not be observed under the condition that $[O_2^-]_0 < 0.1[Fe^{3+}\text{–EDTA}]$. Stoichiometric reaction is precisely what would be predicted from the ratio of k_4 ($= 2 \times 10^6$ M^{-1} s^{-1}) to k_5 ($\sim 2 \times 10^6$ M^{-1} s^{-1}) when [Fe^{3+}–EDTA] $\gg$ [Fe^{2+}–EDTA] and O_2^-.

(71) Diguiseppi, J.; Fridovich, I. *Arch. Biochem. Biophys.* **1980**, *203*, 145–150.